Numerical study on discharge characteristics influenced by secondary electron emission in capacitive RF argon glow discharges by fluid modeling*

Lu-Lu Zhao(赵璐璐)[1,2], Yue Liu(刘悦)[1,†], and Tagra Samir[1]

[1] Key Laboratory of Materials Modification by Laser, Ion and Electron Beams (Ministry of Education), School of Physics, Dalian University of Technology, Dalian 116024, China

[2] School of Information Science and Engineering, Dalian Polytechnic University, Dalian 116034, China

(Received 18 August 2017; revised manuscript received 12 October 2017; published online 5 January 2018)

A one-dimensional (1D) fluid model of capacitive RF argon glow discharges between two parallel-plate electrodes at low pressure is employed. The influence of the secondary electron emission on the plasma characteristics in the discharges is investigated numerically by the model. The results show that as the secondary electron emission coefficient increases, the cycle-averaged electric field has almost no change; the cycle-averaged electron temperature in the bulk plasma almost does not change, but it increases in the two sheath regions; the cycle-averaged ionization rate, electron density, electron current density, ion current density, and total current density all increase. Also, the cycle-averaged secondary electron fluxes on the surfaces of the electrodes increase as the secondary electron emission coefficient increases. The evolutions of the electron flux, the secondary electron flux and the ion flux on the powered electrode increase as the secondary electron emission coefficient increases. The cycle-averaged electron pressure heating, electron Ohmic heating, electron heating, and ion heating in the two sheath regions increase as the secondary electron emission coefficient increases. The cycle-averaged electron energy loss increases with increasing secondary electron emission coefficient.

Keywords: RF glow discharge, secondary electron emission, fluid model

PACS: 52.20.–j, 52.25.–b, 5.25.Jm, 52.30.–q **DOI:** 10.1088/1674-1056/27/2/025201

1. Introduction

Capacitive RF glow discharges at low pressure have been widely adopted in many fields, such as microelectronics and material processing technology. Material processing technology with enhanced secondary electron emission (SEE) is adopted in various applications, such as electronic materials and nanomaterials. In order to improve the efficiencies of these applications, it is very important to understanding the generating mechanism and physical characteristics of the plasmas.

As is well known, the SEE is the emission of the electrons from the electrode surfaces, which occurs mainly when the accelerated ions collide with the electrodes. It leads to the SEE being one of the critical parameters in determining the magnitude of the glow discharge yield.[1–19] Its process under ion bombardment plays an important role in the plasma parameters such as electron density, electron temperature, electric field and potential, and ion and electron heating.[20–31] Many efforts have been made to explore the effect of SEE coefficient γ.[11–20] In the simulations and experiments of RF glow discharge studies, the effect of SEE coefficient γ on the sheath structure is very important, since the electron heating on the electrode surfaces is limited by the electric potential.[4] As the SEE increases, the sheath potential becomes smaller and its isolation effect of primary electron heating from the plasma to the electrode becomes weaker. The theoretical predictions concern the role of the electron heating at the sheath boundary in RF glow discharges, due to the oscillating sheath. The transition of the sheath structure can be controlled by increasing SEE.[4,5] The studies indicate that the sheath heating of the electrons could be the dominant heating mechanism in RF glow discharges, compared with the secondary electron heating.[23–25,31] Though these studies illustrate the discharge mechanisms with considering secondary electrons, the effect of SEE coefficient on the electron heating mechanism or on the discharge sustaining mechanism, which is a key question of RF glow discharge, has not been studied carefully.

In glow discharges, the mechanism of the electron heating largely depends on a wide range of discharge conditions such as electrode gap, gas pressure, driving frequency, applied voltage, etc.[18–23,29,30] Two mechanisms for the electron heating have been observed in the glow discharge: the electron pressure heating and the electron Ohmic heating. A few studies evaluated how effective the electron pressure heating is. The electron Ohmic heating is a continuous process, and the advantages of the electron Ohmic heating are as follows: i) the electrons can be heated homogeneously, and ii) the electrons with low thermal conductivity can also be heated. The SEE

*Project supported by the National Natural Science Foundation of China (Grant No. 51172101).

†Corresponding author. E-mail: liuyue@dlut.edu.cn

© 2018 Chinese Physical Society and IOP Publishing Ltd

coefficient strongly affects ionization in glow discharge. In this paper, the effects of SEE coefficient on the electric field, electric potential, and electron temperature are studied. Also the SEE coefficient as a significant discharge parameter affects greatly on ion heating and electron heating, which consists of electron pressure heating and the electron ohmic heating.

In this work, a one-dimensional (1D) fluid model is used to study the effect of SEE coefficient on the RF glow discharge characteristics. The glow discharge is operated between two parallel plate electrodes. It is assumed that the electrode gap space is much smaller than the electrode diameter. Therefore, a 1D fluid model is reasonable.

The rest of this paper is organized as follows. In Section 2, the model is described. In Section 3, the results from the simulation are discussed. From our calculation results, we find that for all the parameters we choose in this work, after the 5000th cycle, the RF discharge reaches a steady state. Finally, some conclusions are drawn from the present study in Section 4.

2. Model

In our model, a plasma of an RF glow discharge between two parallel-plate electrodes is described. When there exists a certain electric potential difference between the electrodes, the gas discharge between the electrodes will take place and the plasma will be generated. For a better study, we make several assumptions as follows.[31]

(i) The diameters of the electrodes are each much greater than the spacing between the two electrodes. Thus the discharge characteristics change only along the x axis.

(ii) The equations of continuity are written for the electron and ion density, the moment equations are obtained by the integrating Boltzmann equation over velocity space. The continuity equations are coupled to the Poisson equation relating the potential field to the particle density. The electron energy distribution is Maxwellian.

(iii) The diffusivity and mobility of ions and electrons can be described as continuum properties, i.e., continuity equations describe the creation, loss, and transport of charge carriers. Also both the ion flux and electron flux are described by the drift and diffusion approximation. By using a driving frequency of 13.56 MHz and a pressure of more than 100 mTorr (1 Torr = 1.33322×10^2 Pa), the momentum transfer collision frequency is more than the RF driving frequency. So the drift and diffusion approximation is valid.

(iv) Only the ground state ionization is considered, neither the metastable atoms nor any reactions with metastable atoms are taken into account.

(v) The temperatures of ions and neutral particles are constant and equal to gas temperature. Because of the inertia, ions cannot make a quick response to the change of electric field, i.e., ions can obtain little energy from the applied field.

The capacitively coupled RF argon glow discharge at low pressure is simulated. In the discharge, only the inelastic press for particles is considered: $\mathrm{e}+\mathrm{Ar}\rightarrow\mathrm{Ar}^{+}+2\mathrm{e}$.

Thus, the densities of the electrons and the ions satisfy the following equations:

$$\frac{\partial n_\mathrm{e}}{\partial t}+\frac{\partial J_\mathrm{e}}{\partial x}=k_I n_\mathrm{n} n_\mathrm{e}, \tag{1}$$

$$\frac{\partial n_\mathrm{i}}{\partial t}+\frac{\partial J_\mathrm{i}}{\partial x}=k_I n_\mathrm{n} n_\mathrm{e}, \tag{2}$$

$$J_\mathrm{e}=-D_\mathrm{e}\frac{\partial n_\mathrm{e}}{\partial x}-\mu_\mathrm{e} n_\mathrm{e} E, \tag{3}$$

$$J_\mathrm{i}=-D_\mathrm{i}\frac{\partial n_\mathrm{i}}{\partial x}+\mu_\mathrm{i} n_\mathrm{i} E, \tag{4}$$

where J_e and J_i are the fluxes of the electrons and the ions within the drift-diffusion approximation; D_e, D_i, μ_e, and μ_i are the diffusion coefficients and the mobilities of the electrons and the ions, respectively; n_n is the density of neutral atoms of gas and can be written as $n_\mathrm{n}=3.22\times10^{16}p$ (cm^{-3}), with p being the pressure of neutral gas in units of Torr. The terms on the right-hand side in Eqs. (1) and (2) mean that in the source term, only the grounded ionization is considered. For the argon discharge, the ionization rate can be written as

$$k_I=1.235\times10^{-7}(\mathrm{cm}^3\cdot\mathrm{s}^{-1})\exp\left(-18.687(\mathrm{eV})/T_\mathrm{e}\right), \tag{5}$$

where T_e is the electron temperature in units of eV. The electron energy balance is evaluated by

$$\frac{\partial}{\partial t}\left(\frac{3}{2}n_\mathrm{e}kT_\mathrm{e}\right)=-\frac{\partial q_\mathrm{e}}{\partial x}+P_\mathrm{c}-H_I S, \tag{6}$$

$$q_\mathrm{e}=-K_\mathrm{e}\frac{\partial T_\mathrm{e}}{\partial x}+\frac{5}{2}kT_\mathrm{e}J_\mathrm{e}, \tag{7}$$

$$K_\mathrm{e}=\frac{3}{2}kD_\mathrm{e}n_\mathrm{e}, \tag{8}$$

$$P_\mathrm{c}=-eJ_\mathrm{e}E, \tag{9}$$

where q_e is the conductive heat flux of electron energy, K_e is the thermal conductive coefficient, P_c is the electron heating coming from the electron current coupled with the electric field as seen in Eq. (9). The last term on the right-hand side in Eq. (6) is the electron energy loss due to the ionization. The electron heating coming from the electron current has two parts: one is the electron heating coming from the electron pressure and the other is the electron heating coming from the ohmic heating, i.e.,

$$P_\mathrm{c}=P_p+P_\mathrm{h}, \tag{10}$$

where

$$P_\mathrm{p}=eD_\mathrm{e}\frac{\partial n_\mathrm{e}}{\partial x}E, \tag{11}$$

$$P_\mathrm{h}=e\mu_\mathrm{e}n_\mathrm{e}E^2. \tag{12}$$

In this work, P_p is the electron pressure heating, P_h is the electron ohmic heating, and P_c is the electron heating. The electric field satisfies

$$-\frac{\partial^2 V}{\partial x^2} = \frac{e}{\varepsilon_0}(n_i - n_e), \tag{13}$$

$$E = -\frac{\partial V}{\partial x}, \tag{14}$$

where e is the elementary charge and ε_0 is the vacuum permittivity of free space.

The initial conditions we used in this work are as follows:[28,31]

$$n_i = n_e = n_\varepsilon \left[\varepsilon + 16\left(1-\frac{x}{d}\right)^2\left(\frac{x}{d}\right)^2\right],$$
$$T_e = T_{ei}, \quad V = 0, \quad 0 \le x \le d,$$

where n_ε is the peak value of the initial charged particle densities, ε is a small positive number, and d is the gap between the parallel-plate electrodes.

The boundary conditions are as follows.[28,31]

at $x = 0$ (on the powered electrode):

$J_i = \mu_i n_i E$, $J_e = -k_s n_e - \gamma J_i$, $T_e = T_{eb}$, and $V = V_A \sin(2\pi f t)$;

at $x = d$ (on the grounded electrode):

$J_i = \mu_i n_i E$, $J_e = k_s n_e - \gamma J_i$, $T_e = T_{eb}$, and $V = 0$,

where γ and k_s are the SEE coefficient and electron recombination coefficient, respectively.

3. Results and discussion

In order to understand the plasma characteristics with SEE coefficients of 0.01, 0.1, 0.2, and 0.3 in CCRF glow discharge between parallel-plates electrodes, we numerically solve the model by a finite difference method with the boundary conditions and the initial conditions. The parameters used in the simulation are shown in Table 1.

Table 1. Parameters used in the numerical simulation.

Name	Symbol	Value	Ref.
Electron diffusivity	$n_n D_e$	3.86×10^{22} cm^{-1}·s^{-1}	[31]
Electron mobility	$n_n \mu_e$	9.66×10^{21} V^{-1}·cm^{-1}·s^{-1}	[31]
Ion diffusivity	$n_n D_i$	2.07×10^{18} cm^{-1}·s^{-1}	[31]
Ion mobility	$n_n \mu_i$	4.65×10^{19} V^{-1}·cm^{-1}·s^{-1}	[31]
Electron recombination coefficient	k_s	1.19×10^{7} cm·s^{-1}	[31]
Electron energy-loss coefficient	H_I	15.7 eV	[31]
Gas pressure	p	1 Torr	
Gap between the electrodes	d	2.5 cm	
Peak RF voltage	V_A	100 V	
Electron temperature at the electrodes	T_{eb}	0.5 V	
Driving frequency	f	13.56 MHz	

Figure 1 shows the variations of cycle-averaged electric field, electron temperature, ionization rate, and electron density with SEE coefficient, at three positions: in the powered sheath at $x = 0.02$ cm, in the centre of discharge at $x = 1.25$ cm, and in the grounded sheath at $x = 2.48$ cm. Figure 1(a) shows that the electric field almost does not change with increasing SEE coefficients from 0.01 to 0.3. The electric field is virtually constant (zero) in the centre of discharge at $x = 1.25$ cm with all SEE coefficients. Figure 1(b) shows the cycle-averaged electron temperature changing with SEE coefficient increasing. It can be seen that the electron temperature in the centre of the discharge is almost constant for all SEE coefficients. While the electron temperature increases greatly in the two sheath regions compared with in the bulk plasma region as the SEE coefficient increases. This is because the secondary electrons gain high energy inside the sheath region, but these secondary electrons are unable to infiltrate to the bulk plasma region because the mean free path of electron is small under the present conditions.[31] Figure 1(c) shows the changes of the cycle-averaged ionization rate with SEE coefficient in a range from 0.01 to 0.3. The results show that the ionization rate has a significant change in discharge as the SEE coefficient increases; it has much higher change in the sheath region than in the bulk plasma region. The ionization rate is defined as the product of the electron density and the collision frequency between the electrons and neutral atoms. Although the electron densities in the two sheath regions are much smaller than in the bulk plasma region, but the electric fields in the two sheath regions are much larger than in the bulk plasma region. Therefore, as the SEE coefficient increases, the electrons in the two sheath regions can obtain more energies and the collision frequency between the electrons and the neutral atoms is very large, which leads to the larger ionization rates in the two sheath regions. Thus, the electrons before moving into the small ionization region, can generate more and more ionization rate in the sheath region.[16,18] Figure 1(d) shows that the higher electron density occurs in the centre of discharge as the SEE coefficient increases. The electric field slightly increases compared with the large increase of the electron density. The increasing electron density is consistent with the increase of electron temperature and the decrease of sheath thickness slightly as the SEE coefficient increases.[31]

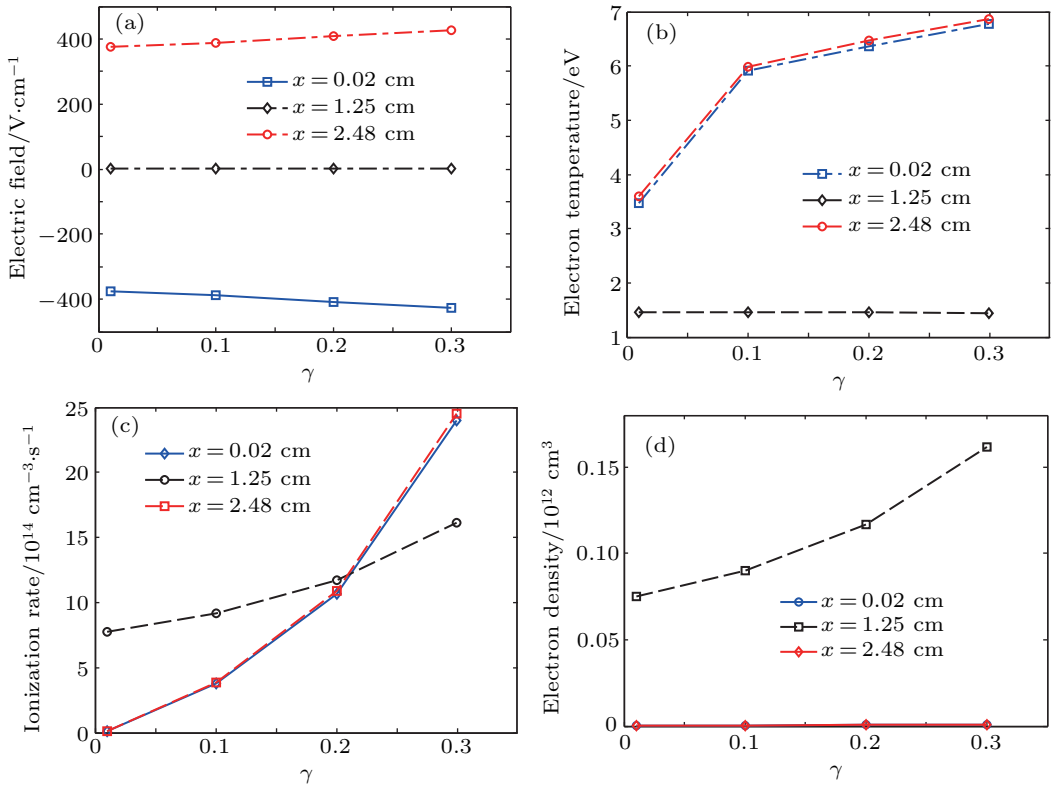


Fig. 1. (color online) Cycle-averaged (a) electric field, (b) electron temperature, (c) ionization rate, and (d) electron density, with SEE coefficient of 0.01, 0.1, 0.2, and 0.3 at three positions: in the powered sheath at $x = 0.02$ cm, in the center of discharge at $x = 1.25$ cm, and in the grounded sheath at $x = 2.48$ cm in the 5000th cycle.

Figure 2(a) gives the variations of cycle-averaged electron current density with x for the SEE coefficients of 0.01, 0.1, 0.2, and 0.3, respectively. It shows that the electron current density is positive in the powered sheath region and negative in the grounded sheath region, according to the electric field negative and positive values. The electron current density is very low in the center of the discharge because the electric field is very weak in the center of the discharge. The sign of the electric field changes when it goes from the powered electrode to the grounded electrode. The electron current density rapidly decreases at the location of low electric field in the sheath region. With the increasing of the SEE coefficient, the electron current density increases and has a peak in the powered sheath region. In the grounded sheath region, the electron current density also increases negatively and has a peak. This is due to the curvatures of the electric field lines in these regions. In the grounded sheath region, where the ion current density positively increases, so there are no ions emitted from the surface. It is clear that the electron current density plays a basic role in sustaining the RF discharge.

Figure 2(b) shows that the cycle-averaged ion current density negatively increases with the increasing of SEE coefficient in the powered sheath region. In the grounded sheath region, the ion current density increases positively as the SEE coefficient increases. It can be explained as follows. Owing to the high electric field and large electric field variations in the sheath region, the energy gained by the electrons from the electric field is not locally balanced by the energy loss through collisions, so that a significant electron flux of high-energy electrons can enter into the negative flow, the powered electrode acts as an electron gun. On the powered electrode, the fall energy gained from the electric field is much larger than the energy loss due to the collisions, so it is dominant in the negative glow.[23] The more the SEE coefficient increases, the more the ion flux created in the powered sheaths region is. The curve of ion current density has no peak-like electron current density because the ions are further accelerated as they pass through the sheath region.

The total current density is given by $J_{\text{total}} = e(J_{\text{i}} - J_{\text{e}})$. The change of the total current density is because the distribution of the electric field in the discharge is strongly affected in the presence of charge particles. But the electric field can also reach quite a large value in the range as indicated in Fig. 1(a) and does not depend on the total current density in the considered range as shown in Fig. 1(a). The cycle-averaged total current density is shown in Fig. 2(c). It should be noted that the total current density changes with SEE coefficient. The figure shows that the total current density is lower and negatively increases in the powered sheath region. In the grounded sheath region, the total current increases positively as SEE coefficient increases.

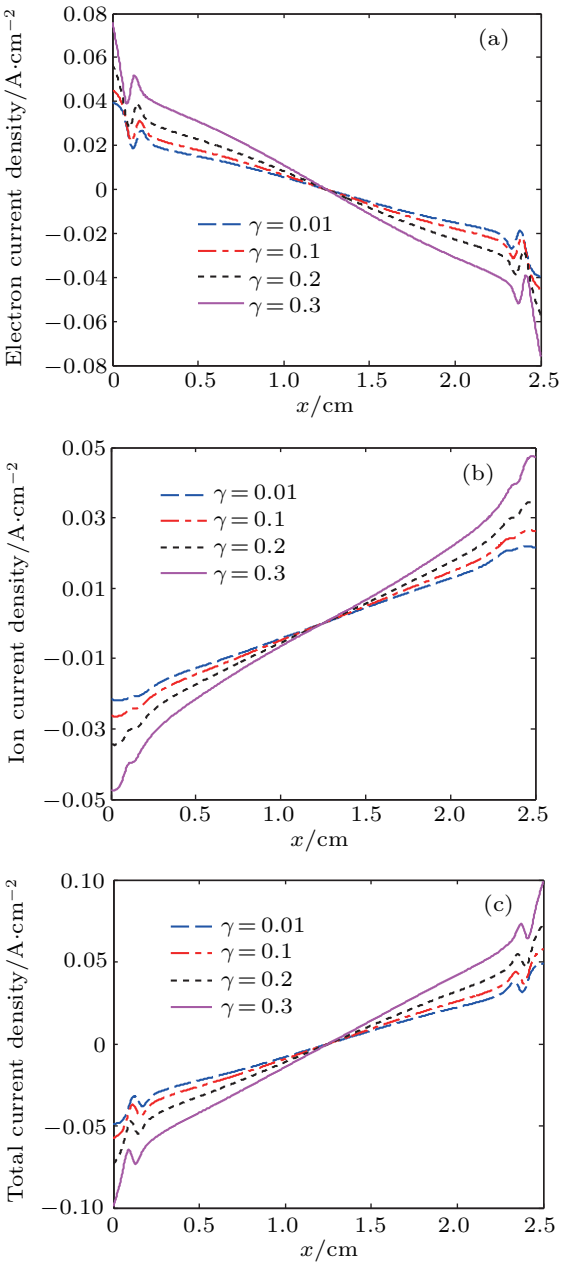


Fig. 2. (color online) Cycle-averaged (a) electron current density, (b) ion current density, (c) total current density, with the SEE coefficients of 0.01, 0.1, 0.2, and 0.3 in the 5000th cycle, respectively.

The secondary electrons flux on the surface of electrode is given by $J_{SE} = -\gamma J_i$. Figure 3 shows the cycle-averaged secondary electron fluxes as a function of the SEE coefficient. Firstly, at a position of $x = 0.00$ cm on the surface of the powered electrode, the electron current is positive and increases as the SEE coefficient increases, so more ohmic heating may take place there. At the same location, the ion current is negative and increases negatively as the SEE coefficient increases. Secondly, the secondary electron flux is negative on the surface of the grounded electrode, because the electron current increases negatively, while the ion current increases positively as the SEE coefficient increases. In the bulk plasma region the electron flux and the ion flux go through zero.[3,4,16]

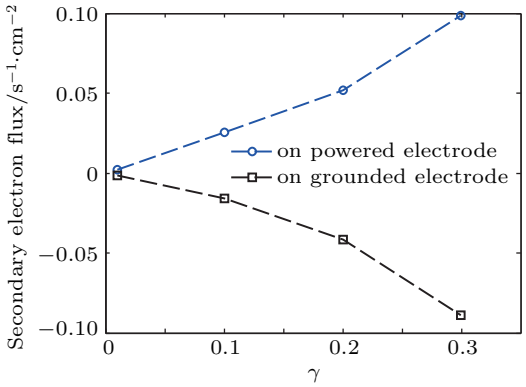


Fig. 3. (color online) Evaluations of secondary electron flux on the surface of the powered electrode at 0.00 cm and grounded electrode at 2.5 cm, as a function of the SEE coefficient in the 5000th cycle.

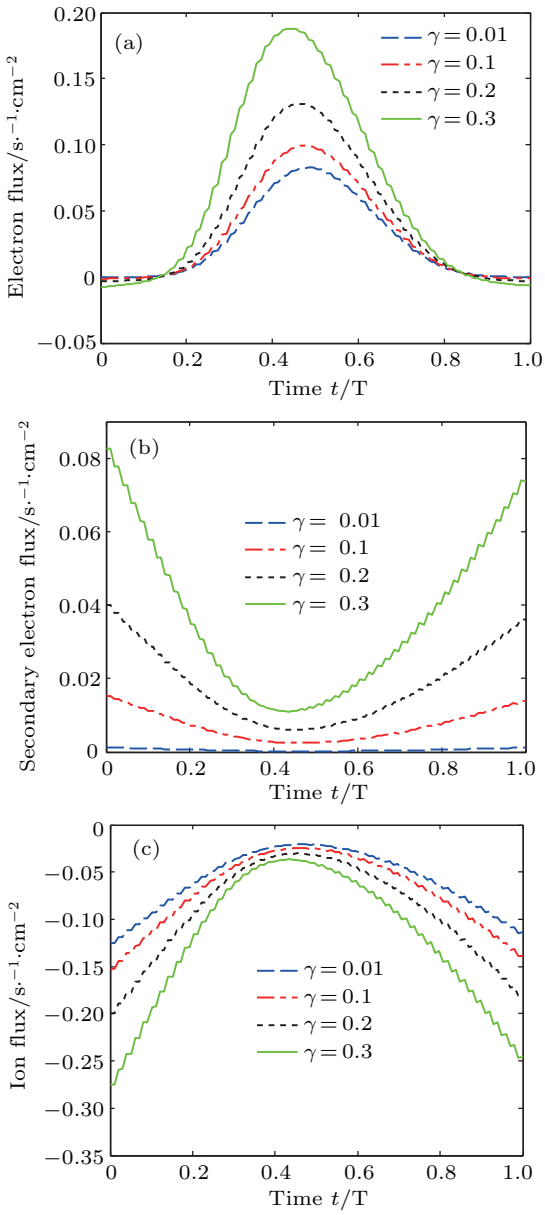


Fig. 4. (color online) Evolutions of (a) electron flux, (b) secondary electron flux, and (c) ion flux on the surface of powered electrode, with the SEE coefficients of 0.01, 0.1, 0.2, and 0.3 in the 5000th cycle, respectively. The letter T in abscissa axis represents period (or cycle).

The evolutions of the electron flux, secondary electron

flux, and ion flux on the surface of the powered electrode in one cycle are shown in Fig. 4. From Fig. 4(a), the electron fluxes increase slowly from negative to zero in the time range from 0 t/T to 0.15 t/T, quickly from zero to positive in the time range from 0.15 t/T to 0.45 t/T; the electron fluxes decrease quickly from positive to zero in the time range from 0.45 t/T to 0.85 t/T, slowly from zero to negative in the time range from 0.85 t/T to 1 t/T. The evolution of the electron flux decreases with increasing SEE coefficient in the time ranges from 0 t/T to 0.15 t/T and from 0.815 t/T to 1.0 t/T. In the time range from 0.15 t/T to 0.815 t/T, the evolution of the electron flux increases largely as the SEE coefficient increases. It can be explained as follows: at the time of maximum sheath voltage, the secondary electrons are created on the surface of the electrode and more ionizations are observed in the sheath region. Meanwhile the electric field becomes stronger inside the sheath region. From Fig. 4(b), the secondary electron fluxes decrease quickly in the time range from 0 t/T to 0.45 t/T and increase quickly in the time range from 0.45 t/T to 1.0 t/T. The evolution of the secondary electron flux increases with increasing SEE coefficient. In the beginning and the end of one cycle, the evolution of the secondary electron flux increases largely with increasing SEE coefficient. From Fig. 4(c), the instantaneous ion flux increases quickly from 0 t/T to 0.45 t/T and decreases quickly from 0.45 t/T to 1.0 t/T. The evolution of the ion flux increases negatively with increasing SEE coefficient.

The electron pressure heating is mainly due to the electron diffusion.[23] Figure 5(a) shows that the cycle-averaged electron pressure heating increases with increasing SEE coefficient and mainly occurs in the sheath region. There are two negative peaks of the electron pressure heating in both sheath regions, and the peaks increase negatively as the SEE coefficient increases. According to Eq. (11), it is easy to find that electrons diffuse along the negative gradient direction of the electron density and move along the negative direction of the electric field. When these electrons reach the centre of discharge, where the electric field becomes low, they would not be cooled any more. In the bulk plasma region, the electron pressure heating is almost constant as the SEE coefficient increases.

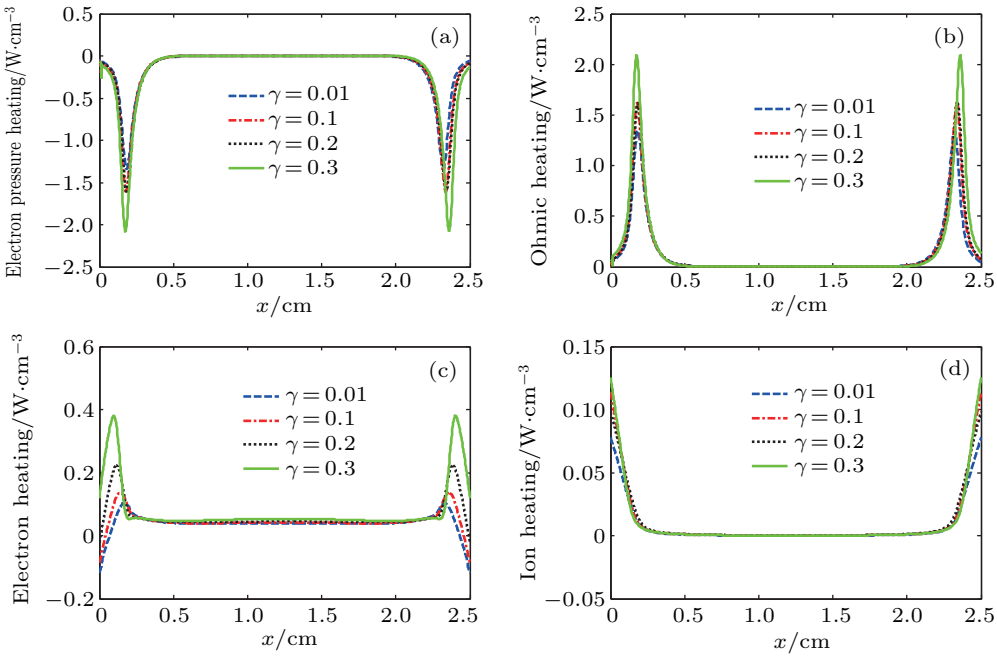


Fig. 5. (color online) Cycle-averaged spatial distributions of (a) electron pressure heating, (b) electron Ohmic heating, (c) electron heating, and (d) ion heating, with the SEE coefficients of 0.01, 0.1, 0.2, and 0.3 in the 5000th cycle, respectively.

The electron Ohmic heating is directly proportional to the square of the electric field, coupling with the electron density as can be seen in Eq. (12). The electric field is varied by adjusting the electrode gap, varying SEE coefficient or applying RF-voltage and frequency.[22] The electric field and electron density increase with temperature rising. It is suggested that the electron Ohmic heating becomes more effective with increasing SEE coefficient, which could theoretically result in escaping electron heating. From Fig. 5(b), it is worth noting that the higher electron Ohmic heating occurs in the sheath region and increases with increasing SEE coefficient. But the change of electron Ohmic heating is virtually constant in the plasma region. Also, the results show that the width of the sheath region shifts slightly toward the electrodes as the SEE coefficient increases. The electron Ohmic heating is large in the sheath region because a large number of electrons are accelerated by the electric field in the sheath region compared with in the bulk plasma region.

As described, most electron heating system configurations consists of two mechanisms: the electron pressure heating and the electron Ohmic heating as shown in Eq. (10). With increasing electron Ohmic heating, the chance of collisions between electrons and neutral particles increases, which leads to the growth of electron heating. Figure 5(c) shows the cycle-averaged electron heating. In the plasma region, the electron heating is positive and slightly increases as the SEE coefficient increases. In the two sheath regions, the electron heating is positive and increases as the SEE coefficient increases, except near the electrodes where the electron heating takes the negative values. The negative electron heating can be thought of as "diffusion cooling" since electrons diffuse against the local field in these regions.[23–25,31]

Figure 5(d) shows that the cycle-averaged ion heating changes with SEE coefficient in a range from 0.01 to 0.3. In the two sheath regions, the ion heating has a significant effect and increases as the SEE coefficient increases. But, in the bulk plasma region, the ion heating is almost zero. In the powered sheath region, the ion heating decreases quickly from the powered electrode. Also, in the grounded sheath region, the ion heating decreases quickly from the grounded electrode. The ion heating is positive where the location of ion-ion energy exchange is large because the energy exchange usually is faster than ion heating, and quite a quantity of charges can be produced there. There is a large interaction of the charge with plasma ion species and the interaction causes more ions to be heated. Also, ions are heated due to interactions between the electric field which collides with the sheath.[16–26]

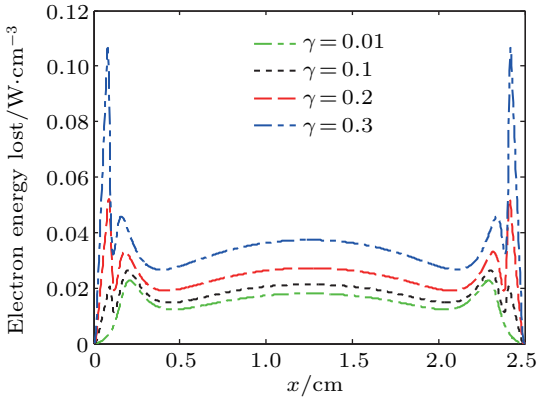


Fig. 6. (color online) Cycle-averaged spatial distributions of electron energy loss, with the SEE coefficients of 0.01, 0.1, 0.2, and 0.3 in the 5000th cycle, respectively.

The cycle-averaged electron energy losses are plotted in Fig. 6 as the SEE coefficient increases. The cycle-averaged electron energy loss occurs in the whole discharge region. The electron energy loss curves each have one peak with SEE coefficient of 0.01 and have two peaks when the SEE coefficient is bigger than 0.01 in the sheath region. It is known that the electrons lose energy as a result of the inelastic collsions between particles and electrons. The electrons gain energy from the electric field and lose energy by their colliding with neutral particles. The electron energy loss depends exponentially on electron temperature but linearly on electron density. It can be seen that as the SEE coefficient increases, the electron energy loss increases more in the bulk plasma region.

4. Conclusions

A 1D fluid model of capacitive RF argon discharge at low pressure is used to study the effect of the effective SEE coefficient γ on the glow discharge characteristics. The evolutions of the discharge parameters are investigated numerically. The results indicate that the electron density increases largely with electric field slightly increasing. Also the electron temperature increases in the two sheath regions and is almost constant in the bulk plasma region. The variations of electron current density between parallel-plate electrodes with the SEE coefficient increasing are presented and compared with each other. The evolutions of the secondary electron flux and the ion flux on the surface of the powered electrode are studied. With the SEE coefficient increasing, the negative maximum of the electron pressure heating in the sheath region increases while it is essentially unchanged in the center of the glow discharge. With SEE coefficient changing from 0.01 to 0.3, there appears a positive maximum of the electron Ohmic heating in each of the two sheath regions, but in the center of the glow discharge, it is almost constant. In addition, the electron heating increases, leading to a corresponding increase of the electron pressure heating and Ohmic heating in glow discharge. The results show that ion heating increases in the two sheath regions. The higher ionization rate and electron energy loss are found in the two sheath regions rather than in the bulk plasma region where it is found to be lower with all SEE coefficients. In general, these numerical results could provide valuable information about electrical glow discharge which otherwise could be determined only by experimental effort.

References

[1] Vahedi V, Birdsall C K, Lieberman M A, Dipeso G and Rognlien T D 1993 *Plasma Sources Sci. Technol.* **2** 273
[2] Vender D and Boswell R W 1990 *IEEE Trans. Plasma Sci.* **18** 725
[3] Lisovskiy V, Martins S, Landry K, Douai D, Booth J P, Cassagne V and Yegorenkov V 2005 *Phys. Plasmas* **12** 093505
[4] Langendorf S and Walker M 2015 *Phys. Plasmas* **22** 033515
[5] Choi E H, Lim J Y, Kim Y G, Ko J J, Kim D L, Lee C W and Cho G S 1999 *J. Appl. Phys.* **86** 6525
[6] Surendra M and Graves D B 1992 *J. Appl. Phys.* **71** 5189
[7] Godyak V A, Piejak R B and Alexandrovich B M 1992 *Plasma Sources Sci. Technol.* **1** 36
[8] Surendra M and Graves D B 1991 *IEEE Trans. Plasma Sci.* **19** 144
[9] Korolov I, Derzsi A, Donkó Z and Schulze J 2013 *Appl. Phys. Lett.* **103** 064102
[10] Yu Q, Deng Y F, Liu Y and Han X W 2008 *Chin. Phys. Lett.* **7** 2569
[11] Phelps A V, Pitchford L C, Pédoussat C and Donkó Z 1999 *Plasma Sources Sci. Technol.* **8** B1
[12] Gogolides E and Sawin H H 1992 *J. Appl. Phys.* **72** 3988
[13] Ohtsu Y and Fujita H 2004 *Phys. Lett.* **85** 4875

[14] Ohtsu Y and Fujita H 2008 *Appl. Phys. Lett.* **92** 171501
[15] Lafleur T, Chabert P and Booth J P 2013 *J. Phys. D: Appl. Phys.* **46** 135201
[16] Schulze J, Donkó Z, Scungel E and Czarnetzki U 2011 *Plasma Sources Sci. Technol.* **20** 045007
[17] Donko Z, Schulze J, Czarnetzki U, Derzsi A, Hartmann P, Korolov I and Schungel E 2012 *Plasma Physics and Controlled Fusion* **54** 124003
[18] Godyak V A and Piejak R B 1990 *Phys. Rev. Lett.* **65** 996
[19] Lieberman M A and Godyak V A 1998 *IEEE Trans. Plasma Sci.* **26** 955
[20] Turner M M 1995 *Phys. Rev. Lett.* **75** 1312
[21] Gozadinos G, Vender D, Turner M M and Lieberman M A 2001 *Plasma Sources Sci. Technol.* **10** 117
[22] Schulze J, Heil B G, Luggenholscher D, Brinkmann R P and U Czarnetzki 2008 *J. Phys. D: Appl. Phys.* **41** 195212
[23] Boeuf J P and Belenguer P 1992 *J. Appl. Phys.* **71** 4751
[24] Belenguer P and Boeuf J P 1990 *Phys. Rev. A* **41** 4447
[25] Boeuf J P 1987 *Phys. Rev. A* **36** 2782
[26] Park S K and Economou D J 1990 *J. Appl. Phys.* **68** 3904
[27] Chen G and Raja L L 2004 *J. Appl. Phys.* **96** 6073
[28] Lymberopoulos D P and Economou D J 1993 *J. Appl. Phys.* **73** 3668
[29] Cluggish B P and Munson C P 1998 *J. Appl. Phys.* **84** 5945
[30] Lafleur T, Chabert P and Booth J P 2014 *Plasma Sources Sci. Technol.* **23** 035010
[31] Liu Q, Liu Y, Samir T and Ma Z S 2014 *Phys. Plasmas* **21** 083511